

# Image Processing of Dermoscopic Images

LEBiom

Principles of Biosignals and Biomedical Imaging

Ana Rita Damas Mendes, 99641, Mariana Vila Flor da Costa, 99703

**Abstract**—Skin cancer is one of the most prevalent types of cancer that has been increasing in recent decades. It is very common to confuse malignant tumours with benign lesions such as keratosis-like lesions, using traditional diagnostic methods. Thus, our aim is to conduct a computational analysis of the skin lesions and, according to their characteristics, split them in two clusters by performing k-means clustering method. It is known, a priori, that of the 10 images 5 are malignant and 5 are benign. The clusters were classified in agreement with the usual features of each type of lesion, considering the ABCDE rule. For this, we implemented a classic image processing pipeline that included the images conversion to grayscale and their inversion, noise removal with a Gaussian filter, thresholding to obtain binary masks and removal of the imperfections in the structure through morphological operations. Then, the features of interest (circularity and standard deviation of intensity distribution) were extracted which allowed the division of the observations in 2 clusters well defined: one associated with lower circularity and higher standard deviation that we classified as the malignant lesions and the other the opposite that we classified as benign lesions, according to literature. We concluded that K-means algorithm was a suitable choice for this project due to its simplicity and effectiveness in dividing the data into two clusters although we consider that a supervised learning algorithm could be a better approach since it improves the performance of the classifier.

## 1 INTRODUCTION

CANCER is undoubtedly one of the deadliest diseases worldwide. Of all types of cancer, skin cancer is among the most prevalent, with its incidence increasing significantly over the past decades. Although melanoma, a malignant type of skin cancer, is much less prevalent than non-melanoma skin cancer, it causes the majority of deaths. [1] [2]

Seborrheic keratoses are common epidermal skin tumors in middle-aged and older patients. These lesions are benign and due to its nature, treatment is often not required. These are often confused with other conditions once they have some morphological similarities with malignant skin lesions. Such mistakes can have serious consequences for the patient, since they might be getting ineffective treatments. For this reason, it is essential to properly differentiate these lesions from other ones, especially malignant skin tumors.[3] [4]

In order to educate patients on how to self-identify suspicious lesions, ABCDE rule is

often recommended mainly for his simplicity and ease to learn. The letters stand for characteristics of malignant transformation: Asymmetry, Border irregularity, Color variability, Diameter of 6 mm or more and Evolving (a new or changing lesion taking in account size, shape, shade of colour, growth rate, surface features or symptoms). [5] [6] However, the rule is flawed since ABCDE features might be found in benign lesions, such as seborrheic keratosis, and are sometimes absent in early melanoma. [5]

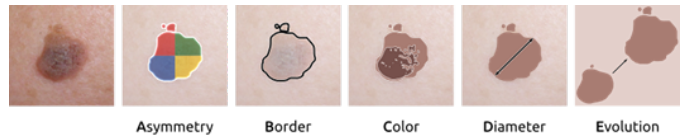


Figure 1: ABCDE rule [9]

Others methods, such as dermoscopy and biopsies, are used by dermatologists in the diagnosis of skin cancer but these are associated with some limitations: dermoscopy usu-

ally only diagnoses accurately when the lesion is clearly malignant, even with the unaided eye, which consequently limits diagnosis of very early and mainly featureless melanomas [7]; biopsies are time-consuming and require extra human effort and use of resources. Given skin cancer's incidence and prevalence, development of fast, cost-effective, and specific diagnoses are thus required.

Having in mind this problematic, this project aims to develop a classification method for skin lesions images, based on parameters namely lesion circularity and intralesional color variation. We will be using K-means clustering method which is one of the simplest unsupervised machine learning algorithms, since our input is not labeled. So, data is evaluated to identify similarities, patterns, and differences among them and is then accordingly grouped into clusters. In this method the Euclidean distance between an observation and the cluster centroid is calculated and data is assigned to the closest cluster. In essence, data is split in k clusters (k is defined initially) in a way to reduce the within-cluster sum of squares.[8]

## 2 STATE-OF-THE-ART

The basic steps to process dermoscopy images analysed in computer-aided diagnosis of skin lesions include image pre-processing, segmentation, extraction of peculiar features, and classification, that distinguishes between cancerous and non-cancerous skin lesions, or types of skin cancer.[10]

### 2.1 Pre-processing

The skin lesion image contains several artifacts such as hair, air bubbles, ink markings, black frames, noise, and uneven illumination, which must be localized and abstracted or replaced in pre-processing, to facilitate the following steps. Some other approaches that have been used are masking, image resizing, filtering and colour space conversions.[10]

In order to get a better visualization of the lesion, it is mostly used the blue channel of RGB image, but in a few cases, it can also be used gray level image. There have been some

works that investigate a more opportune colour space to improve the differentiation between the lesion and the skin surrounding it.[10]

Concerning the problem of uneven illumination, a recent study developed a model based on adaptive bilateral decomposition and polynomial curve fitting to correct illumination variation.[11]

Another relevant aspect is hair removal, which can be resolved by several methods such as Dull Razor software (despite removing only thin hair and making the lesion hazy), that performs morphological operation, bi-linear interpolation, and adaptive median filtering.[12][10]

Some morphological operations include dilation, which turns objects more visible and fills small holes in it, and erosion, which removes floating pixels and thin lines.[13]

Furthermore, it is used filters to smooth and abstract artifacts from the image, like median filters, that preserves some noise and details and are better than Dull Razor to remove thick hair, and weighted mean filters (such as gaussian filter).[12][10]

### 2.2 Segmentation

After pre-processing, segmentation is performed to divide the image into distinct regions to find out the area of interest (skin lesion) by isolating this area from the healthy area (healthy skin surrounding the lesion). Due to unclear borders of the images of skin lesions, this task reveals itself as challenging, leading to the development of several segmentation techniques.[14]

One of the traditional techniques is thresholding, in which pixels with intensities less than a determined threshold value are placed in one category, and the rest are placed in the other category, making it a good method for high contrast images that is able to convert grayscale images into binary images. Otsu's technique, for example, considers every potential value for the threshold between background and foreground, calculates the variance within the two clusters, and chooses the value with the smallest weighted sum of these variances.[10][13]

Furthermore, edge and region-based methods are commonly used for perceiving irregularities in images. Some common examples of edge detectors include Canny (that presents low error and avoids double edges), Sobel, Perwitt and Laplacian. The Laplacian filter is a derivative filter that finds areas of fast intensity shift to locate edges in pictures. Region-based filters segment an image based on the similarity of intensity values between spatially neighbouring pixels.[10][13][15]

Others traditional techniques include water shed segmentation and K-means clustering.[14]

It is also relevant to refer that segmentation of skin lesion images has been greatly facilitated by deep learning methods. [14]

### 2.3 Feature extraction and Classification

Feature extraction improves the accuracy of learned models by extracting features from the input data, reducing it to more manageable groups for processing.[16]

There are various features that can be extracted from dermoscopic images, such as shape features (like Asymmetry Index and circularity index, to measure asymmetry, and least, greatest, normal, and variance responses of the slope administrator applied on the intensity image, to measure lesion border irregularity); colour features (like standard deviation of RGB channels and relative chromaticity); texture features (like coarseness, contrast and directionality); and high-level features (like granularity).[10]

Some algorithms were developed based on feature extraction, such as patter analysis, which detects melanocytic lesions and their level of malignancy based on patterns in the skin image, ABCD rule, Menzies method, Seven-point checklist and CASH.[10]

Ultimately, the gathered traits are utilized in classification methods in order to determine the specific type of skin cancer, or the benignity, exhibited in a skin lesion image. Several conventional classification techniques and algorithms are employed, such as the Naive Bayesian Algorithm, Total Dermoscopy Score (TDS), k-Nearest Neighbors Classifier (k-NN),

SVM, and ANN Classifiers. The primary methods for classification include supervised, semi-supervised, unsupervised (like K-means clustering), reinforcement, evolutionary learning, deep learning, and active learning.[14]

## 3 METHODS

In order to divide the images in 2 groups and classify them, we implemented a classic image processing pipeline:

### 3.1 Dataset

To import the image dataset, two functions were needed: *ImageDatastore*, allowed the creation of a datastore with all images; *Readall* allowed reading all the image files from the datastore and keep them in a cell array named images. The functions *rgb2gray* and *imcomplement* were used to, respectively, convert the images into grayscale and invert them. As a way to simplify the code, a for loop was done to perform the operations in all images at once. This method was used in all steps of methodology.

### 3.2 Denoising

Each image was filtered with a Gaussian filter using *imgaussfilt* with default sigma of 0.5.

### 3.3 Thresholding

The goal of this section is to obtain binary masks where the lesion is white, and the background is black. Using Otsu's method, *graythresh* determines a global threshold from grayscale images. This value as well as the grayscaled, inverted, denoised image were used as arguments of the function *imbinarize* which creates binary masks.

### 3.4 Morphological Operations

Operations including binary dilation and erosion (applying a square structuring element), border clearing, small object removal and hole-filling were performed to remove the imperfections in the structure of image.

### 3.5 Feature Extraction

Firstly, we multiplied each of the grayscaled and inverted images obtained initially with the correspondent binary ones obtained after the morphological operations, in order to get intralesion variation of color intensity. It was necessary to convert the binary values into uint8.

Then, standard deviation and circularity were calculated for each image by using the functions *std2* and *regionprops*, respectively, saving the values in array v (standard deviation) and w (circularity). Since we aimed to determine the standard deviation of color intensity within the lesion, only pixels different from 0 were considered for the calculation.

### 3.6 Data Visualization and Analysis

Here, given the matrix with vectors v and w as columns and the instruction to divide the observations into 2 clusters, *kmeans* enabled image classification in one of the 2 groups. Finally, using *gscatter*, it was possible to visualize in 2D plane the clusters spatial division and each image label (Benign/Malign). The class attribution was based on research done previously.

## 4 RESULTS AND DISCUSSION

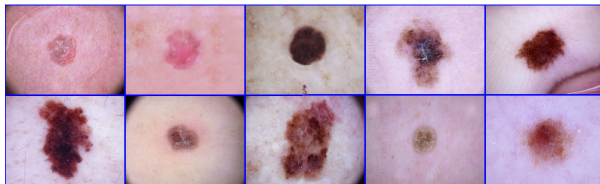


Figure 2: Original Dataset.

The dataset provided was composed by 10 dermoscopic images (Fig.2): 5 corresponding to keratosis-like lesions and 5 to melanomas. The images were labeled from 1 to 10 (from left to right and from top to bottom). The differences on shape and colour variation between some lesions are clear so it seems legitimate to use the parameters circularity and intralesion standard deviation of the intensity distribution to separate the lesions in 2 distinctive classes.

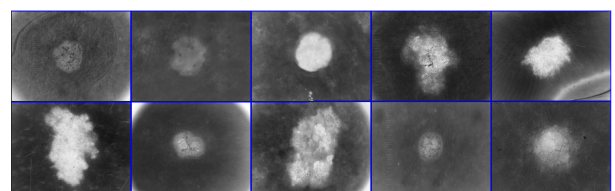


Figure 3: Inverted Gray Scale

As expected, after converting the images into grayscale and invert them, the results are grayscale images with black background and white lesions. This step is convenient for the following methodology since it helps identify edges and other important features and also makes the code simpler that it would be for color images.

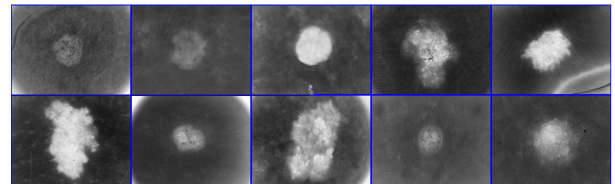


Figure 4: Gaussian filter.

In this step, it was applied a Gaussian smoothing filter, with *imgaussfilt* function, in order to reduce the noise of the images. As it was specified a value of 0.5 (a scalar) for standard deviation, the images in Fig.3 were filtered by a square Gaussian kernel. Since numbers above 0.5 induced a more significant blur, resulting in a cropped lesion image on the threshold step, we opted to maintain the default value of 0.5, obtaining the images on Fig.4. Nevertheless, the differences observed in comparison to the previous images aren't significant.

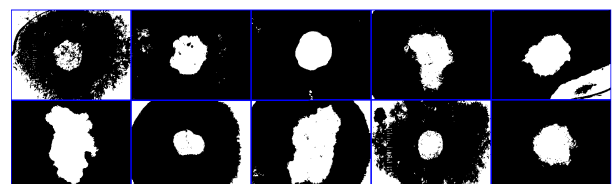


Figure 5: Otsu's method

Using Otsu's method, binary images were obtained, as showed in Fig.5. This technique

finds a threshold from grayscale images that minimizes the intraclass variance of the black and white pixels. Function *graythresh* computes this global threshold that enables the division of the pixels in two clusters: pixels above the threshold are replaced by 1 and the others are replaced with 0. As this method calculates the threshold automatically for each image, it was not necessary to define any parameters.

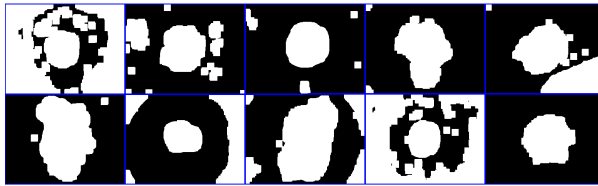


Figure 6: Dilation

In Fig.6, it is observed the addition of pixels to the boundaries of objects, which enables a better visualization of images' details. After testing several sizes and 2D-geometries for the structuring element used in *imdilate*, it was chosen the one which produced later a better clustering of the images, since it is known *a priori* that there are 5 benign images and 5 malign images. Thereby, it was created a square structuring element whose width is 35 pixels, with function *strel*.

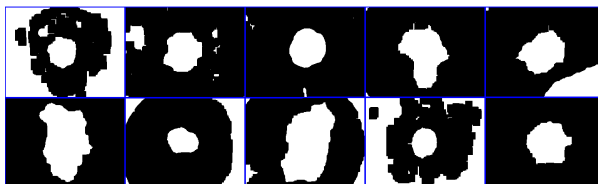


Figure 7: Erosion

In Fig.7, it is used the same structuring element as in dilation, in order to perform a morphological closing. Comparing to Fig.5, it is noted that this process enable the filling of small holes.

To remove the borders of the previous images, it was used function *imclearborder*, with a default connectivity of 8. However, some of the border's pixels remain in the images, predominantly the ones closer to the center of image, since the function used suppresses structures

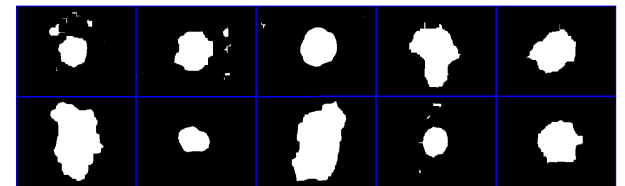


Figure 8: Border Clearing

that are lighter than their surroundings and that are connected to the image border, so the unconnected ones are not eliminated.

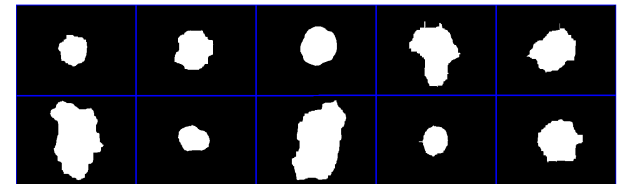


Figure 9: Small Object Removal

To address this issue, it is needed a small object removal step. With function *bwareaopen*, we removed objects containing less than 9000 pixels, since this value allows the removal of all the pixels outside the lesion.

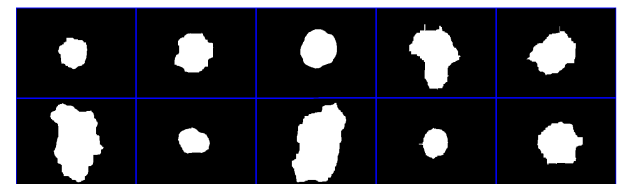


Figure 10: Hole Filling

The hole filling step was useless as there weren't any holes left in the lesion's images, resulting in the same images of Fig.9.

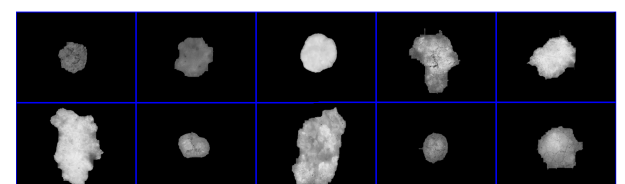


Figure 11: Image obtained by multiplication

Table 1: Standard deviation of intensity distribution

Std Intensity
1. 17.3775
2. 12.1458
3. 18.8995
4. 37.2937
5. 36.5763
6. 32.6018
7. 22.2174
8. 26.4920
9. 22.6698
10. 30.8443

This table presents the standard deviation of the pixel intensity values for each image. By analysing Fig. 11, images 4, 5, 8 and 10 seem to have the biggest intensity variation which is in line with the standard variation values on table 2, where it is possible to observe that the highest value of standard deviation is 37.2937 (image 4) and also that image 6 has a standard deviation of 32.6018, which wasn't expected due to the apparent small variation of pixels' intensity in Fig.11 (first image of second row).

Table 2: Circularity

Circularity
1. 0.7398
2. 0.7034
3. 0.9093
4. 0.4669
5. 0.5573
6. 0.5848
7. 0.8236
8. 0.6080
9. 0.7171
10. 0.6055

Circularity is a measure of the object roundness, with a range of 0 to 1 (maximum circularity). Visually, images 1, 2, 3, 7, 9 are the most circular ones, especially image 3. The circularity values are in agreement with the observed, with a maximum value of 0.9093 correspondent to image 3.

By performing K-means, an output vector containing cluster indices was obtained. This clustering was achieved given the information to partition the observations in 2 groups and taking in account 2 parameters: circularity and std intensity. As std intensity values are a lot bigger than the circularity ones, this variable

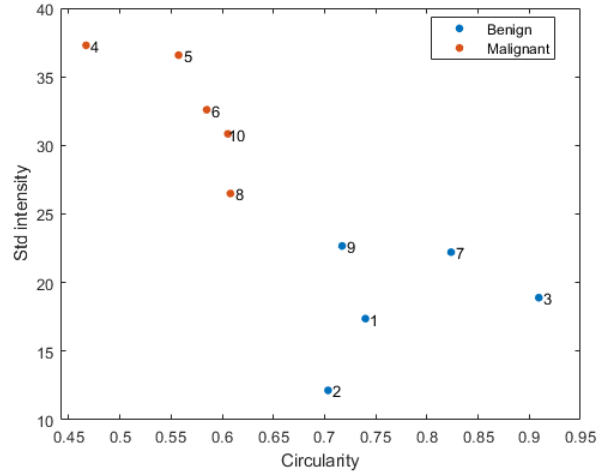


Figure 12: K-means clustering

has greater weight on the centroid calculation and will dominate the measure. This could be avoided with normalization of the data, as will be discussed later.

The graph above shows 2 clusters well defined: one associated with lesions with lower circularity and higher standard deviation of intensity and other the opposite. According to its characteristics and the literature, we decided to classify the first cluster (red dots) as being the malignant lesions once they are usually characterised by irregular borders and intense intralesion colour variation. The second cluster (blue dots) we classified as benign lesion since these have more regular borders and less intralesion colour variation.

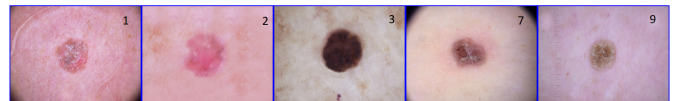


Figure 13: Images in the benign cluster

The images belonging to the benign cluster are in Fig.13. It can be confirmed that they correspond to highly circular lesions with little intralesional colour variation, as expected.

Fig.14 shows images of the malignant cluster in which the asymmetry of the lesion, the irregularity of the border and the high intralesional variability of colour, characteristic of melanomas, are clear.

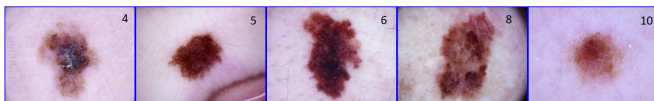


Figure 14: Images in the malign cluster

## 5 CONCLUSION

The objectives proposed initially were accomplished since we were able to partition the images in two clusters by performing K-means and to classify the clusters based on its characteristics and according to literature.

Although the objectives were achieved, the methodology employed could be improved. Image 9 exhibited a subtle protrusion after the morphological operations, so we could have defined the parameters of this image individually in order to get a more accurate border considering the original image. We decided not to do it because the protrusion was really thin, and it seemed not to influence the results. Furthermore, a matrix normalization could be done to ensure that both variables contribute with equal weight for the distance measurement, in a way to optimize the clustering method.

K-means algorithm was a suitable choice for this project due its simplicity and effectiveness in dividing the data into two clusters. Besides that, the advantages of using this algorithm include the ability of finding previously unknown patterns in data and the fact that a train data is not needed. On the other hand, there are also some limitations such as less accuracy and hardship on measuring it since there isn't any predefined answers to compare with. To classify and label the cluster, the user need to spend some time interpreting and researching which represents another drawback. Also, it is non-deterministic until candidate centers are determined: this random behaviour associated with centroid initialization results in different results of the same initial dataset making the method inconsistent and unreliable. Thus, a supervised algorithm would probably be a better approach since it improves the performance of the classifier.

## REFERENCES

- [1] World Health Organization: WHO. (2022, February 3). *Cancer*. <https://www.who.int/news-room/factsheets/detail/cancer>, accessed March 2023.
- [2] World Health Organization: WHO. (2017, October 16) *Radiation: Ultraviolet (UV) radiation and skin cancer*. [https://www.who.int/news-room/questions-and-answers/item/radiation-ultraviolet-\(uv\)-radiation-and-skin-cancer](https://www.who.int/news-room/questions-and-answers/item/radiation-ultraviolet-(uv)-radiation-and-skin-cancer), accessed March 2023
- [3] Izikson, L., Sober, A. J., Mihm, M. C., Zembowicz, A. (2002). Prevalence of Melanoma Clinically Resembling Seborrheic Keratosis. *Archives of Dermatology*, 138(12), 1562. <https://doi.org/10.1001/archderm.138.12.1562>
- [4] Greco, M. J. (2023, February 9). *Seborrheic Keratosis*. StatPearls - NCBI Bookshelf. <https://www.ncbi.nlm.nih.gov/books/NBK545285/>, accessed March 2023
- [5] Duarte, A. R. C., Sousa-Pinto, B., Azevedo, L. F., Barros, A. P., Puig, S., Malvehy, J., Haneke, E., Correia, O. (2021). Clinical ABCDE rule for early melanoma detection. *European Journal of Dermatology*, 31(6), 771-778. <https://doi.org/10.1684/ejd.2021.4171>
- [6] J. D. J., Elewski, B. E. (2015, February). The ABCDEF Rule: Combining the "ABCDE Rule" and the "Ugly Duckling Sign" in an Effort to Improve Patient Self-Screening Examinations. *The Journal of Clinical and Aesthetic Dermatology*, 8(2), 15.
- [7] Skvara, H., Teban, L., Fiebiger, M., Binder, M., Kittler, H. (2005b). Limitations of Dermoscopy in the Recognition of Melanoma. *Archives of Dermatology*, 141(2). <https://doi.org/10.1001/archderm.141.2.155>
- [8] Ecosystem, E. (2018, September 12). *Understanding K-means Clustering in Machine Learning*. Medium. <https://towardsdatascience.com/understanding-k-means-clustering-in-machine-learning-6a6e67336aa1>, accessed March 2023
- [9] IdpMultispectralABCDE.(n.d.). <https://campar.in.tum.de/Students/IdpMultispectralABCDE.html>
- [10] Pathan, S., Prabhu, K. G., Siddalingaswamy, P. C. (2018). *Techniques and algorithms for computer aided diagnosis of pigmented skin lesions—A review*. *Biomedical Signal Processing and Control*, 39, 237-262. <https://doi.org/10.1016/j.bspc.2017.07.010>
- [11] Liu Zhao, Josiane Zerubia, *Skin image illumination modeling and chromophore identification for melanoma diagnosis*, Phys. Med. Biol. 60 (9)(2015) 3415.
- [12] R. Suganya, *An automated computer aided diagnosis of skin lesions detection and classification for dermoscopy images*, 2016 International Conference on Recent Trends in Information Technology (ICRTIT), Chennai, India, 2016, pp. 1-5, doi: 10.1109/ICRTIT.2016.7569538.

[13] MathWorks - Makers of MATLAB and Simulink. (n.d.).  
MATLAB Simulink. <https://www.mathworks.com>

[14] Khattar, S., Kaur, R. (2023). *Computer Aided Diagnosis of Skin Lesion Using Dermoscopic Images: A Survey*. In IOS Press eBooks. IOS Press. <https://doi.org/10.3233/ATDE221320>

[15] ITK:Region-Based Segmentation Filters. (n.d.).  
[https://itk.org/Doxygen/html/group\\_\\_RegionBasedSegmentation.html](https://itk.org/Doxygen/html/group__RegionBasedSegmentation.html)

[16] DeepAI. (2020). Feature Extraction. DeepAI.  
<https://deepai.org/machine-learning-glossary-and-terms/feature-extraction>

## APPENDIX

```

1 %%%
2 % *1) Dataset*
3
4 data=imageDatastore("imagens","FileExtensions",'jpg');
5 images=readall(data);% read all image files from data
6
7 imagesgs=images;%makes a cell array imagesgs,in which we will substitute images with the
8     inverted grayscale images
9 for i=1:10 %for each of the 10 images
10    imagesgs{i,1}=imcomplement(rgb2gray(images{i,1}));%rgb2gray-convert to grayscale;
11    imcomplement-invert array
12    figure,
13    imshow(imagesgs{i,1});%to show the changed image
14 end
15 %%
16 % *2) Denoising*
17
18 sigma=0.5;%standard deviation for imgaussfilt
19 D=imagesgs;%D will contain filtered images(using the previous ones)
20 for i=1:10
21    D{i,1}=imgaussfilt(imagesgs{i,1},sigma);
22    figure,
23    imshow(D{i,1});
24 end
25 %%
26 % *3) Thresholding*
27
28 T=D;%The thresholding(using otsu's method) will be applied on the previous step images.
29 for i=1:10
30    a=D{i,1};
31    T{i,1}=imbinarize(a,graythresh(a));%imbinarize creates a binary image using a threshold;
32    graythresh finds Otsu's threshold.
33    figure,
34    imshow(T{i,1});
35 end
36 %%
37 % *4) Morphological Operations*
38
39 %Binary dilation
40 MO=T;%to apply binary dilation to the previous images(in T)
41 se=strel('square',35);%strel creates a structuring element, in this case a square with 35 of
42     width,in pixels.
43 for i=1:10
44    b=T{i,1};
45    MO{i,1}=imdilate(b,se);%dilates images contained in T, with se(the structuring element)
46    figure,
47    imshow(MO{i,1});
48 end
49 %%
50 %Erosion
51 E=MO;%to apply erosion to the previous images(in MO)
52 for i=1:10
53    c=MO{i,1};
54    E{i,1}=imerode(c,se);%erodes images contained in MO,using the same structuring element as
55    in dilation
56    figure,
57    imshow(E{i,1});
58 end
59 %%
60 %Border clearing
61 BC=E;%to apply border clearing to the previous images(in E)
62 for i=1:10
63    d=E{i,1};

```

```

60 BC{i,1}=imclearborder(d);%suppresses lighter structures connected to the image border, with
61 % a default connectivity of 8.
62 figure,
63 imshow(BC{i,1});
64 end
65 %Removal small objects
66 SOR=BC;
67 P=9000;%to remove small objects in the previous images(in BC)
68 for i=1:10
69 e=BC{i,1};
70 SOR{i,1}=bwareaopen(e,P);%Remove objects containing fewer than P pixels using bwareaopen
function.
71 figure,
72 imshow(SOR{i,1});
73 end
74
75 %Hole filling
76 HF=SOR;%to fill holes in the lesion region of images SOR
77 for i=1:10
78 f=SOR{i,1};
79 HF{i,1}=imfill(f,'holes'); %fills holes in the input image, turning,in this case, black
pixels inside the lesion region to white pixels
80 figure,
81 imshow(HF{i,1});
82 end
83 %%
84 % *5) Feature extraction*
85
86 MT=images;%to create a 10 object cell array, as the images array.
87 for i=1:10
88 MT{i,1}=imagesgs{i,1}.*uint8(HF{i,1});%places in each position of MT the multiplication of
the grayscale obtained image(imagesgs), from the original one, and the image obtained after
morphological operations(HF)
89 figure,
90 imshow(MT{i,1});
91 end
92
93 % Calculate standard deviation
94 v=zeros(10,1);%creates a column array with 10 elements, each equal to zero.
95 for i=1:10
96 imag=double(MT{i,1});
97 imag(imag==0)='';%ignores all the black pixels, corresponding to the background of the
lesion image, to calculate the std2 after.
98 v(i)=std2(imag); %in each element of the array, puts the standard deviation of the
corresponding matrix image(from the previous step).
99 end
100
101 %calculate the circularity of each HF mask.
102 w=zeros(10,1); %to place in the w vector(a column array with 10 zeros) the circularity of each
mask.
103 for i=1:10
104 w(i)=getfield(regionprops(HF{i,1}),'Circularity','Circularity');%The output of regionprops(
measures, in this case, the circularity of mask images-HF) is passed as input to the
getfield function, which retrieves the value of the 'Circularity' field from the structure
returned by regionprops.
105 end
106
107 %%
108 % *6) Data visualization and analyses*
109
110 matriz=[v(:), w(:)]; % creates a 2 column matrix with standard deviation vector(v) and
circularity(w).
111 classes=kmeans(matriz,2) %partitions the points in the matriz into 2 clusters,considering the
minimization of the sum, in each cluster, of the within-cluster sums of point-to-cluster-

```

```
112 centroid distances.  
113 figure,  
114 scatter(w,v); %creates a scatter plot to visualize the 2 clusters formed.  
115 a =[1:10]'; b = num2str(a); c = cellstr(b);  
116 text(w,v,c); %name each point as the corresponding image.  
117  
118 figure,  
119 gscatter(w,v,classes);%scatter plot in which points with the same value of G are shown with the  
    same color.  
120 a =[1:10]'; b = num2str(a); c = cellstr(b);  
121 text(w,v,c);  
122 %montage(BC,'Size',[2 5],'BorderSize', 2, 'BackgroundColor', 'b')->used  
123 %to obtain images in each step of the work(divide in 5 columns and 2 lines)
```